

Explore-and-Match: A New Paradigm for Temporal Video Grounding with Natural Language

Sangmin Woo, Jinyoung Park, Inyong Koo, Sumin Lee, Minki Jeong, Changick Kim
 {smwoo95,jinyoungpark,iykoo010,suminlee94,rhm033,changick}@kaist.ac.kr
 Korea Advanced Institute of Science and Technology (KAIST)

ABSTRACT

Temporal Video Grounding (TVG) aims to localize time segments in an untrimmed video according to natural language queries. In this work, we present a new paradigm named *Explore-and-Match* for TVG that seamlessly unifies two streams of TVG methods: proposal-free and proposal-based; the former *explores* the search space to find segments directly, and the latter *matches* the predefined proposals with ground truths. To achieve this goal, we view TVG as a set prediction problem and design an end-to-end trainable Language Video Transformer (LVTR) that utilizes the architectural strengths of rich contextualization and parallel decoding for set prediction. The overall training schedule is balanced by two key losses that play different roles, namely temporal localization loss and set guidance loss. These two losses allow each proposal to regress the target segment and identify the target query. More specifically, LVTR first *explores* the search space to diversify the initial proposals, and then *matches* the proposals to the corresponding targets to align them in a fine-grained manner. The *Explore-and-Match* scheme successfully combines the strengths of two complementary methods without encoding prior knowledge (e.g., non-maximum suppression) into the TVG pipeline. As a result, LVTR sets new state-of-the-art results on two TVG benchmarks (ActivityCaptions and Charades-STA) with double the inference speed. Code is available at <https://github.com/sangminwoo/Explore-and-Match>.

KEYWORDS

Temporal Video Grounding, Explore-and-Match, Language Video Transformer (LVTR)

1 INTRODUCTION

The explosion of video data brought on by the growth of the internet poses challenges to effective video search. In order to accomplish successful video search, much effort has been put into language query-based video retrieval [9, 12, 30, 48, 49]. While text-video retrieval aims to match a trimmed video clip to the language query, TVG aims to find accurate time segments relevant to the language queries in an untrimmed video. It can be helpful especially when one wants to find a specific scene in a long video, such as a movie. The majority of existing methods for TVG can be categorized into two families: 1) proposal-based methods [2, 5, 13, 14, 17, 25, 26, 33, 43, 45, 48, 50, 54, 56–58], which generate a bunch of proposals in advance and select the best match with target segments, and 2) proposal-free methods [6–8, 15, 29, 31, 36, 42, 45, 52, 53, 55], which estimate start and end timestamps aligned to the given description directly. The proposal-based approaches generally show strong performance at the trade-off of the prohibitive cost of proposal generation. They contradict the end-to-end philosophy, and their performances are

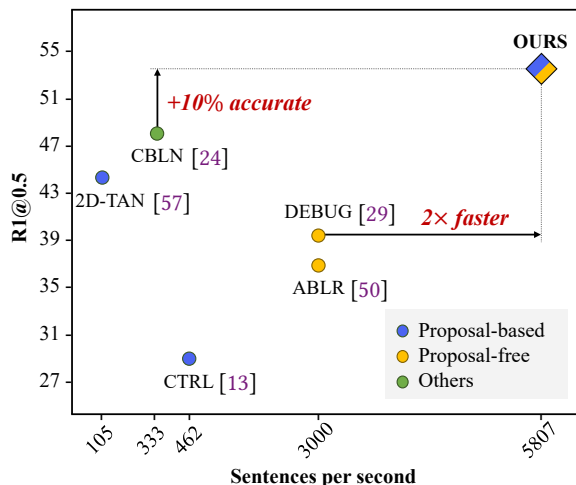


Figure 1: LVTR improves R1@0.5 performance by 10% while being 2× faster than strong baselines on the ActivityCaptions dataset. The average inference speed is measured by the number of localized sentences per second.

significantly influenced by hand-designed pre-processing or post-processing steps such as dense proposal generation [10, 47] or non-maximum suppression [39, 45, 51] to abandon near-duplicate predictions. On the other hand, the proposal-free approaches are much more efficient, but involve difficulties in optimization since the search space for segment prediction is too large.

In this work, we present a new TVG paradigm named *Explore-and-Match* that combines the strengths of the two mainstream approaches by formulating TVG as a direct set prediction problem. Our method keeps the use of proposals while flexibly predicting time segments. Also, it avoids time-consuming pre-processing and post-processing via a direct set prediction. A conceptual comparison of our approach with two previous approaches is shown in Fig. 2. To solve TVG as a set prediction problem, we design an end-to-end trainable model called LVTR based on the transformer encoder-decoder architecture [41]. The primary ingredients of LVTR are bipartite set matching and parallel decoding with a small set of learnable proposals¹. To train all learnable proposals in parallel, we adopt the Hungarian algorithm [21] to find the optimal bipartite matching (i.e., paired in a way that minimizes the matching cost) between ground truths and predictions. This guarantees that each target has a unique match during training. The self-attention mechanism of the transformer enables all elements in an input

¹We refer to trainable positional encodings as *learnable proposals* that are transformed into time segments by the transformer decoder.

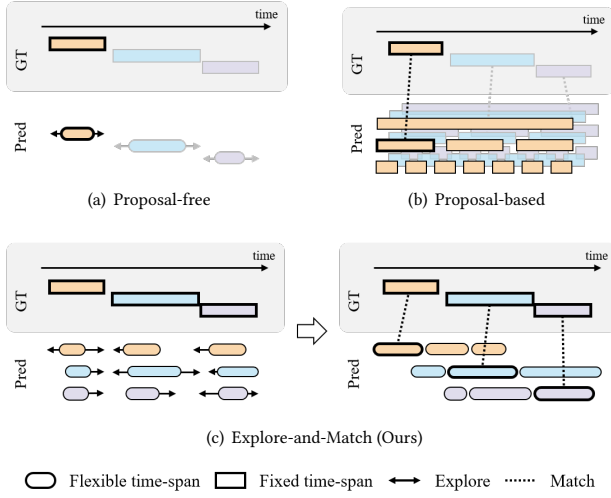


Figure 2: (a) Proposal-free methods directly regress start and end timestamps. (b) Proposal-based methods exhaustively match predefined fixed-size proposals with ground truths. (c) Explore-and-Match paradigm unifies two methods and instead makes flexible time segment proposals. Our method starts with randomly initialized proposals, *explores* time space, and then *matches* the corresponding target.

sequence to interact with one another, making transformer architecture particularly suitable for certain constraints of set prediction, such as suppressing duplicate predictions. By design, LVTR allows us to forgo the use of manually-designed components (e.g., temporal anchors, windows) that encode prior knowledge into the TVG pipelines. Furthermore, learnable proposals can interact with visual-linguistic representations as well as themselves to directly output the final time segment predictions in a single run.

Under the *Explore-and-Match* scheme, the overall training schedule is governed by temporal localization loss and set guidance loss, where the temporal localization loss is responsible for generating accurate time segments, and set guidance loss is responsible for matching predictions with their respective targets (i.e., making target-specific predictions). To match the learnable proposals with their targets, we first divide the learnable proposals by the number of query sentences into several subsets, then set guidance loss progressively forces each subset of proposals to match its corresponding query. In the early stages of training, the temporal localization loss holds the major term in set matching than set guidance loss, which means that it is more of a priority for each subset to somehow approximate the time segment regardless of the target than to predict the corresponding target. Therefore, at first, random subsets learn to reduce temporal localization loss in a target-agnostic manner. Then, once the set guidance loss becomes more dominant than temporal localization loss, the subsets begin to predict each designated target. Finally, all learnable proposals learn to accurately align their respective target segments. Learnable proposals diversify as they *explore* time space, and then *match* their

respective targets. While the training LVTR under the *Explore-and-Match* scheme conforms to the end-to-end basis, it spontaneously divides and conquers the whole process rather than optimizing all the objectives simultaneously. We show the empirical evidence of the *Explore-and-Match* phenomenon (see Fig. 4) and confirm that this simple strategy is remarkably effective (see Fig. 1).

We evaluate LVTR trained under *Explore-and-Match* scheme on two challenging TVG benchmarks — *ActivityCaptions* [3, 20] and *Chrades-STA* [13] — against the recent works. Our LVTR achieves new state-of-the-art results on two benchmarks, even without human priors such as knowledge of time segment distribution. Lastly, we confirm the effectiveness of our approach by conducting extensive ablation studies and analyses. To summarize, our contributions are three-fold:

- We introduce a new TVG paradigm, “*Explore-and-Match*” that unifies the strengths of proposal-based and proposal-free methods.
- We propose an end-to-end trainable model, LVTR, which models the TVG as a set prediction problem. This formulation streamlines the overall pipeline by removing the use of several heuristics.
- Comprehensive experiments and extensive ablation studies demonstrate the effectiveness of LVTR. Moreover, LVTR establishes a new state-of-the-art on two TVG benchmarks while being two times faster than previous methods.

2 RELATED WORK

Temporal Video Grounding. The origin of TVG traces back to the temporal activity localization [37], which attempts to locate the start and end timestamps of actions and identify its labels in an untrimmed video. Likewise, TVG aims to retrieve the corresponding time segments, but it is grounded on language queries rather than a fixed set of action labels. Pioneering TVG works [2, 13] define the task and provide benchmark datasets. Since then, numerous efforts have been made to push the boundaries of TVG. Early works follow the proposal-based pipeline [2, 5, 13, 14, 17, 25, 26, 33, 43, 45, 48, 50, 54, 56–58], which segments a huge number of candidates at regular intervals on different scales, and then ranks them using an evaluation network. While proposal-based approaches provide reliable results, they are highly dependent on proposal quality and suffer from the prohibitive cost of creating proposals, as well as the computationally inefficient comparison of all proposal-target pairings. Another line of works is the proposal-free approaches [6–8, 15, 29, 31, 36, 42, 45, 52, 53, 55], which tries to regress the time segments directly. They are more flexible than proposal-based approaches in terms of granularity. However, its accuracy generally lags behind that of its counterpart. To summarize, the former tries to *match* the predefined proposals with ground truth, while the latter *explores* the whole search space to find time segments directly.

This work aims to integrate two streams of TVG methods into a single paradigm named *Explore-and-Match*, by formulating TVG as a direct set prediction problem. Our method generates flexible time segments like proposal-free approaches while preserving the concept of proposal-based approaches that use positive and negative proposals at the same time.

Transformers. A transformer [41] is a universal sequence processor with an attention-based encoder-decoder architecture. The self-attention mechanism captures both long-range interactions in a single context, and the encoder-decoder attention accounts for token correspondences across multi modalities. Due to the tremendous promise of the attention mechanism, transformers have recently demonstrated their potential in various computer vision tasks: object detection [4], video instance segmentation [46], panoptic segmentation [44], human pose and mesh reconstruction [23], lane shape prediction [27], and human object interaction [59].

Among them, it is worth noting that the Detection Transformer (DETR) [4], the first transformer-based end-to-end object detector, achieved very competitive performance despite its simple design. DETR successfully removes many hand-crafted components from the object detection pipeline by using powerful relation modeling capabilities of transformer. The principal component of DETR is bipartite matching, notably the Hungarian algorithm [21], which generates a set of unique bounding boxes. This saves a lot of post-processing time by removing non-maximum suppression from the pipeline. Also, DETR infers a set of predictions in parallel with a single iteration through the decoder.

Inspired by the recent successes of transformers, we propose a novel TVG model named Language Video Transformer (LVTR) based on the transformer architecture. The attention mechanism of the transformer allows every element of the input sequence to attend to each other while utilizing rich contextualization. This architectural strength makes the transformer particularly suitable for our TVG formulation, a direct set matching problem. We note that final time segment predictions are directly generated in an end-to-end manner.

3 METHOD

We first define the TVG task and propose our end-to-end trainable LVTR. Next, we describe our training losses and set matching strategy. Finally, we present Explore-and-Match, a novel paradigm that unifies proposal-based and proposal-free methods.

3.1 Problem Formulation

TVG aims to localize a set of language-grounded time segments in an untrimmed video. Since TVG does not have a fixed set of sentence classes, the conventional classification approach is not applicable (*i.e.*, taxonomy-free). Therefore, the TVG model should be able to infer the time segments while not being constrained by the predefined categories. Formally, given a video \mathcal{V} with a set of language queries $\mathcal{Q} = \{q_i\}_{i=1}^K$, we require a set of corresponding time segments.

$$\{y_i\}_{i=1}^K = \{(t_i, q_i)\}_{i=1}^K, \quad (1)$$

where $t_i = (t_i^s, t_i^e) \in [0, 1]$ defines the start and end timestamp normalized by the video length (*i.e.*, time segment), and K is the number of the queries. If $K = 1$, the model only expects a single sentence as an input query, which is a conventional single-query setting. In this setting, there is no need for prediction-query assignment since all the predictions of learnable proposals can be associated with only one target (*i.e.*, q_i can be omitted in Eq. (1)). However, this limits the abundant interactions of the transformer with parallel decoding. In order to account for beneficial semantic and temporal

relationships between the time segments, we view TVG as a direct set prediction problem. In a multi-query setting, the model needs to specify which predictions are paired with which queries. Therefore, the grounding model should assign correct queries to the estimated time segments:

$$\{\hat{y}_i\}_{i=1}^N = \{(\hat{t}_i, \hat{q}_i)\}_{i=1}^N, \quad (2)$$

where \hat{t} and \hat{q} denote the predicted time segments and queries, respectively. The number of predictions N is substantially larger than the actual number of queries K in the video.

3.2 LVTR Architecture

The overall pipeline of LVTR is illustrated in Fig. 3. LVTR contains three main components: 1) a feature extractor to obtain compact video and text representations, 2) a transformer encoder-decoder for contextualization and parallel decoding, and 3) a feed-forward network (FFN) that makes the final segment predictions. The architectural details of the LVTR are in the appendix.

Feature Extractor. An input video $\mathcal{V} \in \mathbb{R}^{T_0 \times C_0 \times H_0 \times W_0}$ passes through the C3D [40] (typical values we use are $T_0 = 16, C_0 = 3$ and $H_0 = W_0 = 112$), and is transformed into a video feature $f_v \in \mathbb{R}^{T \times C \times H \times W}$ ($T = 1, C = 512$ and $H = W = 4$). Since the input to transformer encoder should be in the form of sequence, we collapse the channel and spatial dimensions into a single dimension ($T \times CHW$). Then, we feed the output into a linear layer, which yields $T \times D$ dimensions. On the other hand, input language queries \mathcal{Q} break down into a set of word sequences, and then are converted into GloVe [32] embeddings. A set of sentence representations $f_t \in \mathbb{R}^{K \times D}$ ($K \geq 1, D = 512$) is obtained via a 2-layer bi-LSTM [18], followed by a linear layer. The input sentences are batch-processed by applying zero-padding to have the same dimension K as the largest number of sentences within the batch. For a fair comparison, LVTR is equipped with a conventional C3D+LSTM backbone, but it can be trained on top of any modern backbone (*e.g.*, CLIP [34], ViT [11]).

Language Video Transformer. To begin, video and text features are obtained using their respective feature extractors. We concatenate video-text features and pass them into the transformer encoder. The transformer is unable to preserve the order of temporally arranged video features due to the permutation-invariant nature of the architecture. Therefore, we add fixed positional encodings to concatenated video-text features at every attention layer. Each encoder layer has two sub-layers: a multi-head self-attention layer and a feed-forward network. The key component of the encoder is self-attention, which relates different positions of a single sequence to compute an intra-representation of the sequence. The decoder structure adds encoder-decoder attention in addition to the two sub-layers in the encoder. The decoder takes a fixed-size set of N inputs, which we refer to as *learnable proposals*, and decodes them into a set of N output embeddings. All proposals collaboratively generate predictions in a set-wise manner with self-attention while accessing the whole video-text context with encoder-decoder attention. The output embeddings from the decoder are fed into the prediction head, resulting in N final time segment predictions. The prediction head is a 2-layer perceptron with a two-dimensional output, which is set to predict start and end timestamps. To match the proposals

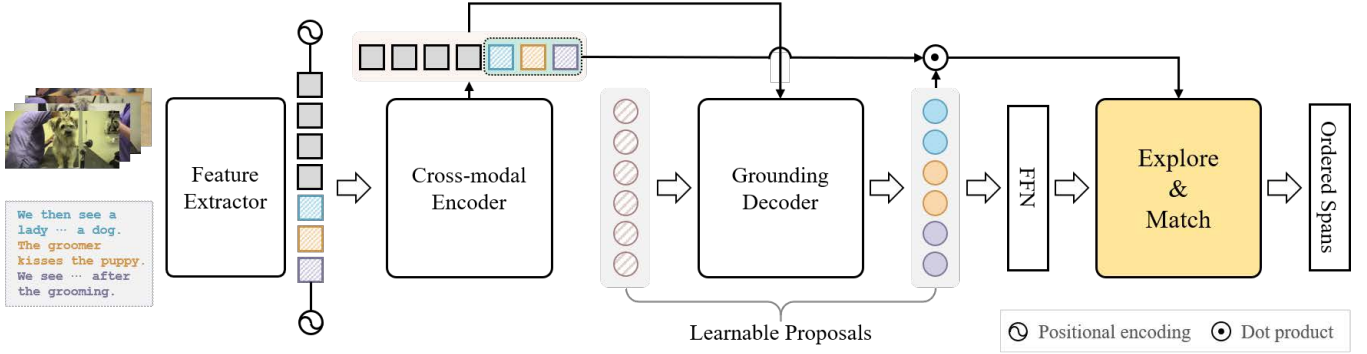


Figure 3: Overview of LVTR. From the feature extractor, we first obtain video and text features and supplement them with positional encoding. The encoder takes as input a sequence of concatenated video-text features. The decoder is fed with a fixed number of *learnable proposals*, which in turn attend to themselves and the encoder output, generating contextualized outputs. These outputs are then used to predict time segments via a FFN and used to measure the correspondence (e.g., normalized similarity) with the textual outputs of the encoder using a dot product (\odot). Following that, the overall training process follow the *Explore-and-Match* scheme (more details are in Fig. 4). The LVTR is trained end-to-end, and it can directly output a set of ordered time segments in parallel.

to corresponding sentences, we measure their correspondence with the normalized similarity of the decoder output and textual output of the encoder. This is used to link each prediction to the query with the highest similarity.

3.3 Explore-and-Match

Considering that video includes multiple events over various periods, we view TVG as a set prediction problem. To solve a set prediction problem between predicted and ground truth time segments, we adopt a Hungarian matching algorithm [21]. We define our loss based on the set matching results. Several training ingredients condense into Explore-and-Match, a new paradigm that combines two streams of methods, proposal-based and proposal-free.

TVG as a set prediction. We search for one-to-one matching between the prediction set $\{\hat{y}_i\}_{i=1}^N$ and the ground truth set $\{y_i\}_{i=1}^K$ that optimally assigns predicted time segments to each ground truth. We assume that the number of predictions N is sufficiently larger than the number of queries K in the video. Therefore, we consider the ground truth set y as a set of size N padded with \emptyset (no matching) for one-to-one matching. We define a set of all permutations that consist of N items as \mathfrak{S}_N . Among the set of permutations \mathfrak{S}_N , we seek an optimal permutation $\hat{\sigma} \in \mathfrak{S}_N$ that best assigns the predictions at the lowest cost:

$$\hat{\sigma} = \underset{\sigma \in \mathfrak{S}_N}{\operatorname{argmin}} \sum_{i=1}^N C_{\text{match}}(y_i, \hat{y}_{\sigma(i)}), \quad (3)$$

where $C_{\text{match}}(y_i, \hat{y}_{\sigma(i)})$ is a pair-wise matching cost between ground truth y_i and a prediction with index $\sigma(i)$. We detail the matching cost in Eq. (8).

Set guidance loss. By the permutation-invariant nature of the transformer, the prediction order cannot be determined. This raises a question: how can we match the predictions with corresponding queries? To address this problem, we introduce a set guidance loss that forces each prediction to be associated with a particular

language query. Given K input queries, N proposals are uniformly partitioned into K subsets. The proposals within the j th subset are trained to predict the j th query by set guidance loss. Formally, we denote the probability that the prediction corresponds to the target query q_i (i.e., softmaxed correspondence) as $\hat{p}_{\sigma(i)}(q_i)$ for the prediction with index $\sigma(i)$. The set guidance loss is simply defined as a negative log-likelihood loss:

$$\mathcal{L}_{\text{sg}}(q_i) = - \sum_i \log \hat{p}_{\sigma(i)}(q_i). \quad (4)$$

While all proposals collaboratively predict a set of time segments via parallel decoding, the set guidance loss leads proposals to predict target-specific time segments.

Temporal localization loss. Our temporal localization loss is a linear combination of the ℓ_1 loss and the generalized IoU (gIoU) loss [35]:

$$\mathcal{L}_{\text{loc}}(t_i, \hat{t}_{\sigma(i)}) = \lambda_{\text{L1}} \mathcal{L}_{\text{L1}}(t_i, \hat{t}_{\sigma(i)}) + \lambda_{\text{IoU}} \mathcal{L}_{\text{IoU}}(t_i, \hat{t}_{\sigma(i)}), \quad (5)$$

where t_i is the ground truth time segment and $\hat{t}_{\sigma(i)}$ is the predicted time segment for the prediction with index $\sigma(i)$. $\lambda_{\text{L1}}, \lambda_{\text{IoU}} \in \mathbb{R}$ are balancing hyperparameters. While two loss terms share the same objective, they have subtle differences. The ℓ_1 loss will have different scales for short and long time segments, even if relative errors are similar, whereas gIoU loss is robust to varying scales.

$$\mathcal{L}_{\text{L1}}(t_i, \hat{t}_{\sigma(i)}) = \|t_i^s - \hat{t}_{\sigma(i)}^s\|_1 + \|t_i^e - \hat{t}_{\sigma(i)}^e\|_1, \quad (6)$$

$$\mathcal{L}_{\text{IoU}}(t_i, \hat{t}_{\sigma(i)}) = 1 - \frac{\min(t_i^e, \hat{t}_{\sigma(i)}^e) - \max(t_i^s, \hat{t}_{\sigma(i)}^s)}{\max(t_i^e, \hat{t}_{\sigma(i)}^e) - \min(t_i^s, \hat{t}_{\sigma(i)}^s)}, \quad (7)$$

where t^s and t^e denote the start and end timestamp, respectively. If two time segments t_i and $\hat{t}_{\sigma(i)}$ perfectly overlap, the loss becomes 0; if they do not overlap at all, the loss becomes greater than 1.

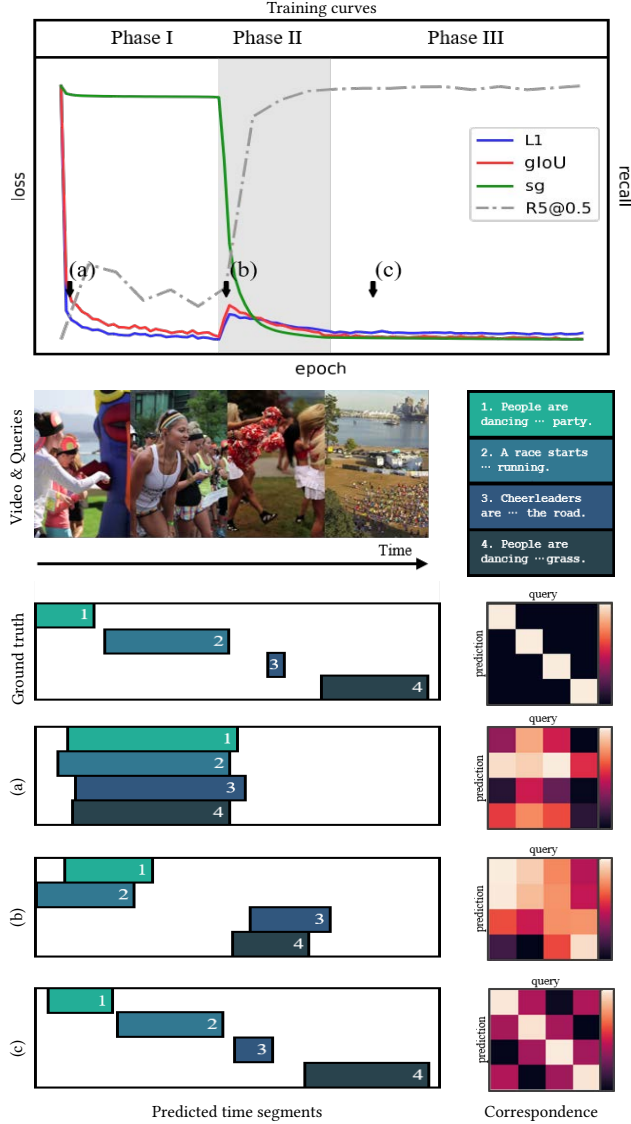


Figure 4: Visualization of time segment predictions (left) and prediction-query correspondences (right) at three different points along the training curves (top): (a) At early training, neither segments nor order is accurate. (b) During the search space exploration, the segments are in the process of aligning with the targets, but they are unordered. (c) After proposals match the corresponding targets, the predicted segments are accurately aligned with the paired targets.

Final set prediction loss. The target query prediction and time segment prediction are factored into the matching cost. We define matching cost using these notations:

$$C_{match}(y_i, \hat{y}_{\sigma(i)}) = -\mathbb{1}_{\{q_i \neq \emptyset\}} \hat{p}_{\sigma(i)}(q_i) + \mathbb{1}_{\{q_i \neq \emptyset\}} \mathcal{L}_{loc}(t_i, \hat{t}_{\sigma(i)}), \quad (8)$$

where $\mathbb{1}$ indicates the indicator function. Here, we consider the K matched predictions as positives (i.e., $q_i \neq \emptyset$), and the remaining $(N - K)$ predictions as negatives (i.e., $q_i = \emptyset$). Contrary to the loss, we do not use the negative log-likelihood for the set guidance loss, but rather approximate it to $1 - p_{\sigma(i)}(q_i)$. We omit a constant 1 since it does not change the matching. Based on the matching results, our final set prediction loss is defined as:

$$\mathcal{L}_{set}(y, \hat{y}) = \sum_{i=1}^N [\lambda_{sg} \mathcal{L}_{sg}(q_i) + \mathbb{1}_{\{q_i \neq \emptyset\}} \mathcal{L}_{loc}(t_i, \hat{t}_{\sigma(i)})], \quad (9)$$

where λ_{sg} is a loss coefficient. Only the positives are optimized to predict the corresponding ground truth time segments.

Unifying two streams of methods. Our approach inherits only the advantages from the proposal-based and the proposal-free methods. We use the proposals, the core concept of the proposal-based methods, to encourage positive proposals to have higher similarities and suppress the negative proposals to have lower similarities with ground truth. However, since proposal-based methods view TVG as a classification problem, their performances are largely limited by hand-crafted components, such as predefined anchors and windows. Our approach differs from the proposal-based methods in that it incorporates the flexibility of proposal-free methods. We make every proposal learnable, allowing them to be fine-tuned within the training pipeline and dynamically transformed into more reliable proposals without the need for heuristics.

The combination of training ingredients condenses into a novel learning paradigm named Explore-and-Match. As shown in Fig. 4, the set guidance loss and the temporal localization loss tend to show different patterns in training curves, where the former generates a cliff-like loss curve and the latter degrades smoothly. At the beginning of the training (Phase I: Fig. 4(a)), predicted time segments are almost a random initialization without order. Before the sharp drop of a set guidance loss (Phase II: Fig. 4(b)), a set of time segments aligns with a set of ground truths in a target-agnostic manner. Interestingly, as the set guidance loss decreases, the ℓ_1 loss and gIoU loss rebound slightly to reorganize predictions to be target-specific. When all losses converge (Phase III: Fig. 4(c)), time segments become accurate to match the target query. We empirically found that our method leads proposals to explore the search space, and then try to accurately match the target. We note that the whole process is carried out in a systematic and holistic manner.

4 EXPERIMENTS

We first describe our experimental settings. Next, we report our main results on two challenging benchmarks: *ActivityCaptions* [3, 20] and *Charades-STA* [13]. Lastly, we provide detailed ablation studies on the model variants and losses, and analyze how LVTR works with visualizations. Additional results can be found in the appendix.

4.1 Experimental Setup

Datasets. 1) *ActivityCaptions* [3, 20] contains about 20K untrimmed videos with language descriptions and temporal annotations, which was originally developed for the task of dense video captioning [20]. Following the convention, we used *val*₁ for validation and *val*₂ for testing since the test annotations are not publicly released. We also

followed the standard split [52]. 2) **Charades-STA** [13] is built on Charades [38] and contains 6,672 videos of daily indoors activities. Each video is about 30 seconds long on average. We employed 12,408 video-sentence pairs for train and 3,720 pairs for test.

Evaluation metrics. Following [29, 52], we adopted two standard evaluation metrics for TVG: 1) “ $R\alpha@μ$ ”, which denotes the percentage of test samples that have at least one correct result in top- α retrieved results, *i.e.*, recall; here, the correct results indicate that IoU with ground truth is larger than threshold $μ$. 2) “**mIoU**”, which averages the IoU between predictions and ground truths over entire testing samples to compare the overall performance.

Technical details. We trained LVTR using AdamW [28] with an initial learning rate of 1e-4 and weight decay of 1e-4 for a batch size of 16. We used a linear learning rate decay by a factor of 10. We considered Xavier initialization [16] to set the initial values of all transformer weights. We used 64 frames that are uniformly sampled from video with four sentences as an input. We resized every frame to 112×112. The number of learnable proposals is proportionally set to 10 times the number of input queries. For a fair evaluation with baselines, we extracted video representations with C3D [40] pretrained on Sports-1M [19], and for the language part, we initialized each word with GloVe embeddings [32] and obtained sentence representation via 2-layer bi-LSTM [18]. In training, we set our loss weight $\lambda_{L1} : \lambda_{iou} : \lambda_{sg}$ to 1 : 3 : 2. We also used an auxiliary decoding loss [1] in decoder layers to speed up the convergence. The initial proposals are filled with learnable weights [4].

4.2 Main Results

Comparison with state-of-the-art approaches. We compared LVTR against recently proposed TVG methods, which can be largely categorized into three groups: 1) proposal-based: CTRL [13], TGN [5], 2D-TAN [57], CSMGAN [25], MSA [56], 2) proposal-free: ABLR [52], DEBUG [29], DRN [53], VSLNET [55], CPNET [22], and 3) *etc*: BP-Net [47], CBLN [24]. LVTR with C3D backbone (LVTR-C3D) sets new state-of-the-arts on two benchmarks (see Table 1): *ActivityCaptions* [3, 20] and *Charades-STA* [13]. Especially for R1@0.5 metric on *ActivityCaptions* dataset, LVTR-C3D achieved about 10% performance gain compared to CBLN [24]. We further improved the performance of LVTR by using CLIP [34] as a backbone (LVTR-CLIP) where a massive amount of image-text pairs are pre-trained with contrastive learning. Even freezing the backbone in the training phase, we observed that CLIP significantly boosts the performance, implying that visual-linguistic domain alignment is important.

Inference speed. We compared several methods in terms of inference speed required to localize a single sentence query in Fig. 1. Our LVTR takes an average of 10ms to process a language query on *ActivityCaptions* dataset. LVTR runs much faster than the previous TVG methods, especially 2× faster than DEBUG [29]. Furthermore, our set matching formulation eliminates the time-consuming pre-processing or post-processing stage, such as dense proposal generation and non-maximum suppression.

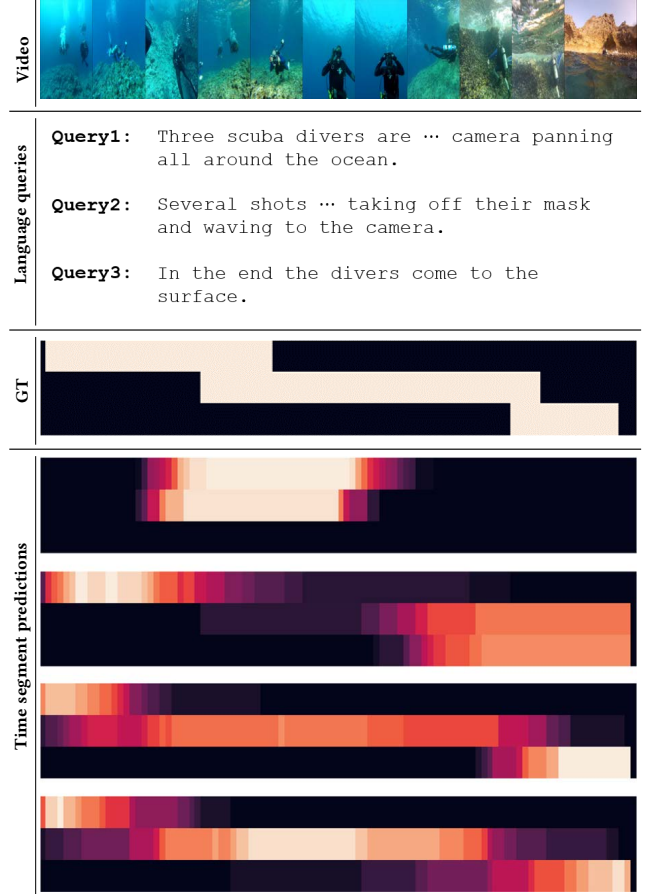


Figure 5: Visualization of time segment predictions throughout training under Explore-and-Match scheme. The four predictions are in time order from top to bottom, where the first two of them show the *explore* process and the last two show the *match* process. The brighter the color, the more time segments predicted by proposals overlap.

4.3 Analysis

Training with Explore-and-Match scheme. In Fig. 5, we investigated the behavior of LVTR during training under the Explore-and-Match scheme. Beginning with the random initialization, the proposals start to generate some variations in their predictions (1st). Thereafter, they become a state in which they can adapt to any time segment by slightly overlapping the boundaries of two ground truths (2nd). Then, each of their identities is determined, and their time segments are adjusted accordingly (3rd). After matching the identity, the proposals properly fit the relevant time segment in a fine-grained manner (4th). To our surprise, despite all training losses are given at once, the training process follows the form of a divide-and-conquer-like approach. We hypothesize that a carefully designed training scheme facilitates this systematic behavior.

Loss ablations. We analyzed the impact of the loss terms in Table 2: ℓ_1 loss (\mathcal{L}_{L1}), gIoU loss (\mathcal{L}_{iou}), and set guidance loss (\mathcal{L}_{sg}). Since matching the target query is essential, we always used set

Table 1: Comparison with the state-of-the-arts on two benchmark datasets: *ActivityCaptions* and *Charades-STA*.

		Venue	<i>ActivityCaptions</i>					<i>Charades-STA</i>				
Methods			R1@0.5	R1@0.7	R5@0.5	R5@0.7	mIoU	R1@0.5	R1@0.7	R5@0.5	R5@0.7	mIoU
proposal-based	CTRL [13]	ICCV2017	-	-	-	-	-	23.63	8.89	58.92	29.52	-
	TGN [5]	EMNLP2018	27.93	-	44.20	-	-	-	-	-	-	-
	2D-TAN [57]	AAAI2020	44.51	26.54	77.13	61.96	-	39.70	27.1	80.32	51.26	-
	CSMGAN [25]	ACMMM2020	49.11	29.15	77.43	59.63	-	-	-	-	-	-
	MSA [56]	CVPR2021	48.02	31.78	78.02	63.18	-	-	-	-	-	-
proposal-free	ABLR [52]	AAAI2019	36.79	-	-	-	36.99	-	-	-	-	-
	DEBUG [29]	EMNLP2019	39.72	-	-	-	39.51	37.39	17.69	-	-	36.34
	DRN [53]	CVPR2020	45.45	24.36	77.97	50.30	-	45.40	26.40	88.01	55.38	-
	VSLNET [55]	ACL2020	43.22	26.16	-	-	43.19	47.31	30.19	-	-	45.15
	CPNET [22]	AAAI2021	40.65	21.63	-	-	40.65	40.32	22.47	-	-	37.36
etc	BPNET [47]	AAAI2021	42.07	24.69	-	-	42.11	38.25	20.51	-	-	38.03
	CBLN [24]	CVPR2021	48.12	27.60	79.32	63.41	-	47.94	28.22	88.20	57.47	-
LVTR-C3D (Ours)			53.27	27.93	78.19	57.82	51.00	47.15	25.72	86.91	53.19	44.26
LVTR-CLIP (Ours)			58.79	33.38	77.47	59.68	53.00	49.11	26.59	88.50	55.99	47.13

Table 2: Ablation results of the loss functions.

\mathcal{L}_{sg}	\mathcal{L}_{L1}	\mathcal{L}_{iou}	R1@0.5	R1@0.7	R5@0.5	R5@0.7	mIoU
✓			24.30	9.60	24.69	9.75	26.9
✓	✓		41.42	18.25	72.55	54.90	41.25
✓		✓	50.15	27.90	72.32	55.50	48.01
✓	✓	✓	58.79	33.38	77.47	59.68	53.00

guidance loss for all cases. When both L1 and gIoU are disabled, the predictions are collapsed; thus, R1@0.5 and R5@0.5 showed almost the same results. When either L1 loss or gIoU loss is disabled, performance suffered significantly, implying that they are both required for accurate temporal localization. As using all three losses yielded the best result, we confirmed that two sub-losses of temporal localization loss (L1 and gIoU) operate complementarily with absolute or relative criteria for time segment prediction.

Correspondence measures. We compared the various measures to calculate the correspondence between prediction and query in Table 3, which is then used in set guidance loss. In practice, we considered proposal-target matching using decoder output and the textual part of encoder output. The encoder-decoder attention weight (Att) is an intuitive way of determining which part of the encoder output each proposal corresponds to. Since it has direct access to the global context, it performed well especially for the R5 metric, but fell short for the rigorous R1 metric. We observed that using cosine similarity (Cos) dramatically improves performance than directly applying dot product similarity (Sim), meaning that removing the size constraint eases optimization.

Positional encodings. In Table 4, we ablated the positional encodings of LVTR. First, we disabled positional encoding for both video and text input. As expected, temporally unorganized input severely degrades performance. The positional encoding of each modality input is then removed in turn. When the video positional

Table 3: Choices for pred-query correspondence measure.

Methods	R1@0.5	R1@0.7	R5@0.5	R5@0.7	mIoU
Sim	13.11	2.75	13.15	2.79	23.73
Att	34.36	18.10	82.42	63.31	39.16
Cos	58.79	33.38	77.47	59.68	53.00

encodings are disabled, the model can no longer utilize temporally coordinated video contexts. Also, the temporal clue provided by textual positional encoding is significant in textual input since it aids in organizing the order of events. We used both positional encodings since both positional encoding largely contributes to the performance. To align the video and text in a different time axis, we employed separate positional encodings for each modality input.

Model size. To examine the effect of model size, we varied the number of encoder-decoder layers (see Table 5). We first compared the two asymmetric structures (#Enc-#Dec): 2-1 vs. 1-2. Compared to the former, the latter falls 2.18 points in R5@0.5 and 6.33 points in R5@0.7 metrics, showing that the contextualization in the encoder is important in generating high-quality proposals. As the size of the transformer increases, the R1 metric gradually improves, while R5 does not change appreciably. This suggests that increasing the size of the transformer has the effect of focusing on selecting better predictions among the candidates. However, considering that the performance degraded in 5-5, stacking more encoder-decoders does not always guarantee higher performance. Among several variants, we found that 4-4 shows the optimal performance.

Number of learnable proposals. We searched for the optimal number of proposals per language query in Table 6. A small number of proposals limits sufficient interactions between positives and negatives, resulting in sub-optimal performance, whereas an excessive quantity of proposals reduces accuracy by generating too

Table 4: Positional encodings.

vid	txt	R1@0.5	R1@0.7	R5@0.5	R5@0.7	mIoU
		25.71	12.69	66.34	41.45	29.85
✓		22.86	10.75	63.95	40.83	30.11
	✓	38.18	16.05	74.56	54.58	40.88
✓	✓	58.79	33.38	77.47	59.68	53.00

Table 5: Model variants w.r.t encoder-decoder size.

#enc	#dec	R1@0.5	R1@0.7	R5@0.5	R5@0.7	mIoU
1	1	48.16	25.55	79.38	64.34	48.02
2	1	48.20	26.08	77.57	64.05	47.67
1	2	48.30	25.40	75.39	57.72	47.97
2	2	55.22	31.13	76.39	61.65	50.99
3	3	53.32	26.62	74.65	58.44	48.92
4	4	58.79	33.38	77.47	59.68	53.00
5	5	56.11	33.82	79.15	60.70	52.04

Table 6: Number of learnable proposals per query.

#proposals	R1@0.5	R1@0.7	R5@0.5	R5@0.7	mIoU
5	48.74	25.40	86.37	70.68	48.03
10	58.79	33.38	77.47	59.68	53.00
15	34.26	16.17	65.59	47.35	39.74
20	6.64	2.16	18.02	6.11	13.07

many negatives. There is a trade-off between R5 and mIoU metrics around the appropriate number of proposals. Between them, having 10 learnable proposals per query yielded the best results.

Qualitative examples & attention visualization. In Fig. A.2, we show a sample TVG result, where the bars lie along the time axis represent the time segments grounded on the query. The predictions (color bars) generated by LVTR nearly matched the target time segments (empty bars). As shown in the proposal-video attention map (bottom), the time segments in which each subset of learnable proposals attend to are mostly overlapped with their corresponding time segment prediction; for example, the third subset attend to the end part of the video. This implies that proposals within the same subset consider similar parts of the video contexts when predicting the target query.

Distribution of learnable proposals. We visualize the time segment predictions of 10 out of all learnable proposals in Fig. 7. We observed that they exhibited a variety of distinct patterns, implying that LVTR learns unique specializations for each proposal. More specifically, each proposal includes several operating modes attending to different time zones and durations. For example, the top-third proposal learned about a long period of time at the beginning of the videos. Overall, all proposals have a mode that predicts video-wide durations, denoted by the color blue.

5 CONCLUSION

We have introduced *Explore-and-Match*, a new TVG paradigm that unifies proposal-based and proposal-free approaches; our approach

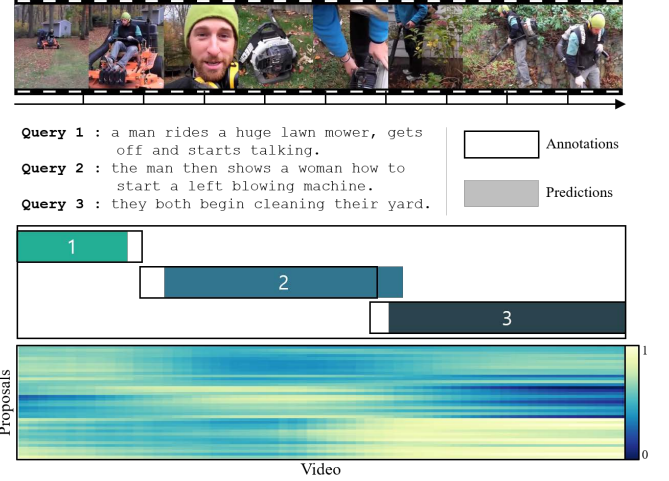


Figure 6: TVG results (middle) of LVTR with proposal-video attention map (bottom). The bottom color map indicates the attention to the video time segment (column) of each proposal (row), where the brighter the color, the higher attention is. Note that each subset of learnable proposals attends to the corresponding video contexts to predict the target time segments.

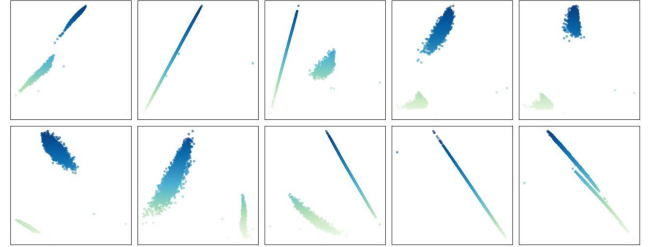


Figure 7: Visualization of predicted time segments on *ActivityCaptions* for 10 out of all learnable proposals. Each prediction is represented by a colored point on the horizontal (center) and vertical (width) axes, where the color indicates the width. We observe that each learnable proposal learns to specialize on certain time zones and durations.

inherits the former concept while proposals are flexible as in the latter. We view TVG as a direct set prediction problem, and design a transformer-based LVTR to solve this problem. LVTR is end-to-end trainable and can predict time segments in parallel by utilizing abundant video-text contexts. We employ bipartite matching in tandem with two key losses: 1) set guidance loss forces to match the target, and 2) temporal localization loss regresses each proposal to fit the corresponding time segment. Our approach diversifies proposals in the *explore* stage, and aligns each learnable proposal with specific target in the *match* stage. LVTR achieve new state-of-the-art results on two challenging benchmarks (ActivityCaptions and Charades-STA) while doubling the inference speed. We hope our exploration and findings facilitate future research on TVG.

REFERENCES

- [1] Rami Al-Rfou, Dokook Choe, Noah Constant, Mandy Guo, and Llion Jones. 2019. Character-Level Language Modeling With Deeper Self-Attention. In *AAAI*, Vol. 33. 3159–3166.
- [2] Lisa Anne Hendricks, Oliver Wang, Eli Shechtman, Josef Sivic, Trevor Darrell, and Bryan Russell. 2017. Localizing Moments in Video With Natural Language. In *ICCV*. 5803–5812.
- [3] Fabian Caba Heilbron, Victor Escorcia, Bernard Ghanem, and Juan Carlos Nibbles. 2015. Activitynet: A Large-Scale Video Benchmark for Human Activity Understanding. In *CVPR*. 961–970.
- [4] Nicolas Carion, Francisco Massa, Gabriel Synnaeve, Nicolas Usunier, Alexander Kirillov, and Sergey Zagoruyko. 2020. End-to-End Object Detection With Transformers. In *ECCV*. Springer, 213–229.
- [5] Jingyuan Chen, Xinpeng Chen, Lin Ma, Zequn Jie, and Tat-Seng Chua. 2018. Temporally Grounding Natural Sentence in Video. In *EMNLP*. 162–171.
- [6] Long Chen, Chujie Lu, Siliang Tang, Jun Xiao, Dong Zhang, Chilie Tan, and Xiaolin Li. 2020. Rethinking the Bottom-Up Framework for Query-Based Video Localization. In *AAAI*, Vol. 34. 10551–10558.
- [7] Shaoxiang Chen, Wenhao Jiang, Wei Liu, and Yu-Gang Jiang. 2020. Learning Modality Interaction for Temporal Sentence Localization and Event Captioning in Videos. In *ECCV*. Springer, 333–351.
- [8] Shaoxiang Chen and Yu-Gang Jiang. 2020. Hierarchical Visual-Textual Graph for Temporal Activity Localization via Language. In *ECCV*. Springer, 601–618.
- [9] Shizhe Chen, Yida Zhao, Qin Jin, and Qi Wu. 2020. Fine-Grained Video-Text Retrieval With Hierarchical Graph Reasoning. In *CVPR*. 10638–10647.
- [10] Zhenfang Chen, Lin Ma, Wenhan Luo, Peng Tang, and Kwan-Yee K Wong. 2020. Look Closer To Ground Better: Weakly-Supervised Temporal Grounding of Sentence in Video. *arXiv preprint arXiv:2001.09308* (2020).
- [11] Alexey Dosovitskiy, Lucas Beyer, Alexander Kolesnikov, Dirk Weissenborn, Xi-aohua Zhai, Thomas Unterthiner, Mostafa Dehghani, Matthias Minderer, Georg Heigold, Sylvain Gelly, et al. 2020. An Image Is Worth 16x16 Words: Transformers for Image Recognition at Scale. *arXiv preprint arXiv:2010.11929* (2020).
- [12] Valentin Gabeur, Chen Sun, Karteek Alahari, and Cordelia Schmid. 2020. Multi-Modal Transformer for Video Retrieval. In *ECCV*. Springer, 214–229.
- [13] Jiyang Gao, Chen Sun, Zhenheng Yang, and Ram Nevatia. 2017. TALL: Temporal Activity Localization via Language Query. In *ICCV*. 5267–5275.
- [14] Runzhou Ge, Jiyang Gao, Kan Chen, and Ram Nevatia. 2019. Mac: Mining Activity Concepts for Language-Based Temporal Localization. In *WACV*. IEEE, 245–253.
- [15] Soham Ghosh, Anuva Agarwal, Zarana Parekh, and Alexander Hauptmann. 2019. Excl: Extractive Clip Localization Using Natural Language Descriptions. *arXiv preprint arXiv:1904.02755* (2019).
- [16] Xavier Glorot and Yoshua Bengio. 2010. Understanding the Difficulty of Training Deep Feedforward Neural Networks. In *AISTATS*. JMLR Workshop and Conference Proceedings, 249–256.
- [17] Lisa Anne Hendricks, Oliver Wang, Eli Shechtman, Josef Sivic, Trevor Darrell, and Bryan Russell. 2018. Localizing Moments in Video With Temporal Language. *arXiv preprint arXiv:1809.01337* (2018).
- [18] Sepp Hochreiter and Jürgen Schmidhuber. 1997. Long Short-Term Memory. *Neural computation* 9, 8 (1997), 1735–1780.
- [19] Andrej Karpathy, George Toderici, Sanketh Shetty, Thomas Leung, Rahul Sukthankar, and Li Fei-Fei. 2014. Large-Scale Video Classification With Convolutional Neural Networks. In *CVPR*. 1725–1732.
- [20] Ranjay Krishna, Kenji Hata, Frederic Ren, Li Fei-Fei, and Juan Carlos Nibbles. 2017. Dense-Captioning Events in Videos. In *ICCV*. 706–715.
- [21] Harold W Kuhn. 1955. The Hungarian Method for the Assignment Problem. *Naval research logistics quarterly* 2, 1-2 (1955), 83–97.
- [22] Kun Li, Dan Guo, and Meng Wang. 2021. Proposal-Free Video Grounding with Contextual Pyramid Network. In *AAAI*, Vol. 35. 1902–1910.
- [23] Kevin Lin, Lijuan Wang, and Zicheng Liu. 2021. End-to-End Human Pose and Mesh Reconstruction With Transformers. In *CVPR*. 1954–1963.
- [24] Daizong Liu, Xiaoye Qu, Jianfeng Dong, Pan Zhou, Yu Cheng, Wei Wei, Zichuan Xu, and Yulai Xie. 2021. Context-aware Biaffine Localizing Network for Temporal Sentence Grounding. In *CVPR*. 11235–11244.
- [25] Daizong Liu, Xiaoye Qu, Xiao-Yang Liu, Jianfeng Dong, Pan Zhou, and Zichuan Xu. 2020. Jointly Cross-And Self-Modal Graph Attention Network for Query-Based Moment Localization. In *ACMMM*. 4070–4078.
- [26] Meng Liu, Xiang Wang, Liqiang Nie, Qi Tian, Baoquan Chen, and Tat-Seng Chua. 2018. Cross-Modal Moment Localization in Videos. In *ACMMM*. 843–851.
- [27] Ruijin Liu, Zejian Yuan, Tie Liu, and Zhiliang Xiong. 2021. End-to-End Lane Shape Prediction With Transformers. In *WACV*. 3694–3702.
- [28] Ilya Loshchilov and Frank Hutter. 2017. Decoupled Weight Decay Regularization. *arXiv preprint arXiv:1711.05101* (2017).
- [29] Chujie Lu, Long Chen, Chilie Tan, Xiaolin Li, and Jun Xiao. 2019. DEBUG: A Dense Bottom-Up Grounding Approach for Natural Language Video Localization. In *EMNLP-IJCNLP*. 5144–5153.
- [30] Antoine Miech, Dimitri Zhukov, Jean-Baptiste Alayrac, Makarand Tapaswi, Ivan Laptev, and Josef Sivic. 2019. Howto100m: Learning a Text-Video Embedding by Watching Hundred Million Narrated Video Clips. In *ICCV*. 2630–2640.
- [31] Jonghwan Mun, Minsu Cho, and Bohyung Han. 2020. Local-Global Video-Text Interactions for Temporal Grounding. In *CVPR*. 10810–10819.
- [32] Jeffrey Pennington, Richard Socher, and Christopher D Manning. 2014. Glove: Global Vectors for Word Representation. In *EMNLP*. 1532–1543.
- [33] Xiaoye Qu, Pengwei Tang, Zhikang Zou, Yu Cheng, Jianfeng Dong, Pan Zhou, and Zichuan Xu. 2020. Fine-Grained Iterative Attention Network for Temporal Language Localization in Videos. In *ACMMM*. 4280–4288.
- [34] Alec Radford, Jong Wook Kim, Chris Hallacy, Aditya Ramesh, Gabriel Goh, Sandhini Agarwal, Girish Sastry, Amanda Askell, Pamela Mishkin, Jack Clark, et al. 2021. Learning Transferable Visual Models From Natural Language Supervision. *arXiv preprint arXiv:2103.00020* (2021).
- [35] Hamid Rezaeifighi, Nathan Tsoi, JunYoung Gwak, Amir Sadeghian, Ian Reid, and Silvio Savarese. 2019. Generalized Intersection Over Union: A Metric and a Loss for Bounding Box Regression. In *CVPR*. 658–666.
- [36] Cristian Rodriguez, Edison Marrese-Taylor, Fatemeh Sadat Saleh, Hongdong Li, and Stephen Gould. 2020. Proposal-Free Temporal Moment Localization of a Natural-Language Query in Video Using Guided Attention. In *WACV*. 2464–2473.
- [37] Zheng Shou, Dongang Wang, and Shih-Fu Chang. 2016. Temporal Action Localization in Untrimmed Videos via Multi-Stage CNNs. In *CVPR*. 1049–1058.
- [38] Gunnar A Sigurdsson, Gül Varol, Xiaolong Wang, Ali Farhadi, Ivan Laptev, and Abhinav Gupta. 2016. Hollywood in Homes: Crowdsourcing Data Collection for Activity Understanding. In *ECCV*. Springer, 510–526.
- [39] Mattia Soldan, Mengmeng Xu, Sisi Qu, Jesper Tegner, and Bernard Ghanem. 2021. VLG-Net: Video-Language Graph Matching Network for Video Grounding. In *ICCV*. 3224–3234.
- [40] Du Tran, Lubomir Bourdev, Rob Fergus, Lorenzo Torresani, and Manohar Paluri. 2015. Learning Spatiotemporal Features With 3D Convolutional Networks. In *ICCV*. 4489–4497.
- [41] Ashish Vaswani, Noam Shazeer, Niki Parmar, Jakob Uszkoreit, Llion Jones, Aidan N Gomez, Łukasz Kaiser, and Illia Polosukhin. 2017. Attention is All You Need. In *NeurIPS*. 5998–6008.
- [42] Hao Wang, Zheng-Jun Zha, Xuejin Chen, Zhiwei Xiong, and Jiebo Luo. 2020. Dual Path Interaction Network for Video Moment Localization. In *ACMMM*. 4116–4124.
- [43] Hao Wang, Zheng-Jun Zha, Liang Li, Dong Liu, and Jiebo Luo. 2021. Structured Multi-Level Interaction Network for Video Moment Localization via Language Query. In *CVPR*. 7026–7035.
- [44] Huiyu Wang, Yukun Zhu, Hartwig Adam, Alan Yuille, and Liang-Chieh Chen. 2021. Max-DeepLab: End-to-End Panoptic Segmentation With Mask Transformers. In *CVPR*. 5463–5474.
- [45] Jingwen Wang, Lin Ma, and Wenhao Jiang. 2020. Temporally Grounding Language Queries in Videos by Contextual Boundary-Aware Prediction. In *AAAI*, Vol. 34. 12168–12175.
- [46] Yuqing Wang, Zhaoliang Xu, Xinlong Wang, Chunhua Shen, Baoshan Cheng, Hao Shen, and Huaxia Xia. 2021. End-to-End Video Instance Segmentation With Transformers. In *CVPR*. 8741–8750.
- [47] Shaoming Xiao, Long Chen, Songyang Zhang, Wei Ji, Jian Shao, Lu Ye, and Jun Xiao. 2021. Boundary Proposal Network for Two-Stage Natural Language Video Localization. In *AAAI*, Vol. 35. 2986–2994.
- [48] Huijuan Xu, Kun He, Bryan A Plummer, Leonid Sigal, Stan Sclaroff, and Kate Saenko. 2019. Multilevel Language and Vision Integration for Text-To-Clip Retrieval. In *AAAI*, Vol. 33. 9062–9069.
- [49] Xun Yang, Jianfeng Dong, Yixin Cao, Xun Wang, Meng Wang, and Tat-Seng Chua. 2020. Tree-Augmented Cross-Modal Encoding for Complex-Query Video Retrieval. In *SIGIR*. 1339–1348.
- [50] Yitian Yuan, Lin Ma, Jingwen Wang, Wei Liu, and Wenwu Zhu. 2019. Semantic Conditioned Dynamic Modulation for Temporal Sentence Grounding in Videos. *arXiv preprint arXiv:1910.14303* (2019).
- [51] Yitian Yuan, Lin Ma, Jingwen Wang, Wei Liu, and Wenwu Zhu. 2020. Semantic Conditioned Dynamic Modulation for Temporal Sentence Grounding in Videos. *TPAMI* (2020).
- [52] Yitian Yuan, Tao Mei, and Wenwu Zhu. 2019. To Find Where You Talk: Temporal Sentence Localization in Video With Attention Based Location Regression. In *AAAI*, Vol. 33. 9159–9166.
- [53] Runhao Zeng, Haoming Xu, Wenbing Huang, Peihao Chen, Minghui Tan, and Chuang Gan. 2020. Dense Regression Network for Video Grounding. In *CVPR*. 10287–10296.
- [54] Da Zhang, Xiyang Dai, Xin Wang, Yuan-Fang Wang, and Larry S Davis. 2019. Man: Moment Alignment Network for Natural Language Moment Retrieval via Iterative Graph Adjustment. In *CVPR*. 1247–1257.
- [55] Hao Zhang, Aixin Sun, Wei Jing, and Joey Tianyi Zhou. 2020. Span-Based Localizing Network for Natural Language Video Localization. *arXiv preprint arXiv:2004.13931* (2020).
- [56] Mingxing Zhang, Yang Yang, Xinghan Chen, Yanli Ji, Xing Xu, Jingjing Li, and Heng Tao Shen. 2021. Multi-Stage Aggregated Transformer Network for Temporal Language Localization in Videos. In *CVPR*. 12669–12678.

- [57] Songyang Zhang, Houwen Peng, Jianlong Fu, and Jiebo Luo. 2020. Learning 2d Temporal Adjacent Networks for Moment Localization With Natural Language. In *AAAI*, Vol. 34. 12870–12877.
- [58] Zhu Zhang, Zhijie Lin, Zhou Zhao, and Zhenxin Xiao. 2019. Cross-Modal Interaction Networks for Query-Based Moment Retrieval in Videos. In *SIGIR*. 655–664.
- [59] Cheng Zou, Bohan Wang, Yue Hu, Junqi Liu, Qian Wu, Yu Zhao, Boxun Li, Chenguang Zhang, Chi Zhang, Yichen Wei, et al. 2021. End-to-End Human Object Interaction Detection With HOI Transformer. In *CVPR*. 11825–11834.

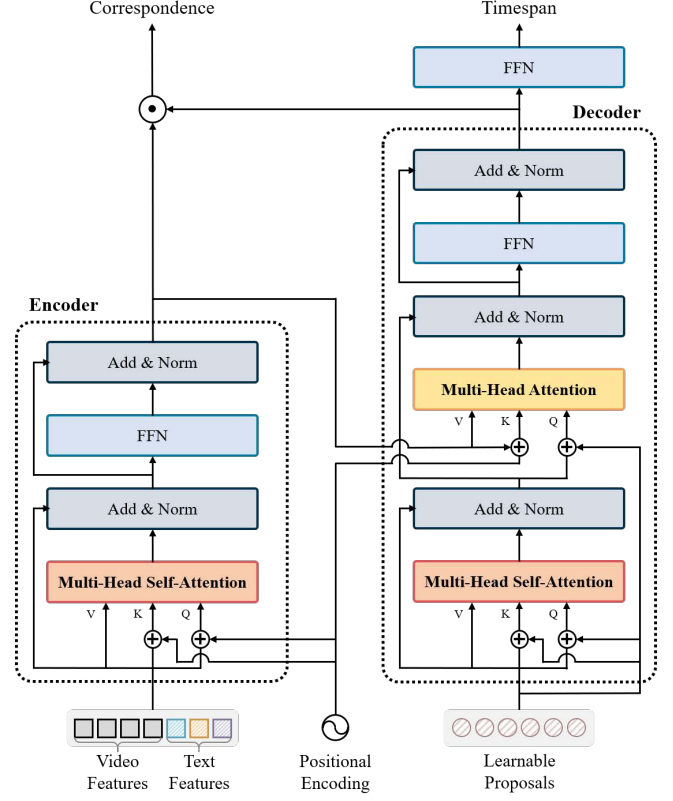


Figure A.1: LVTR Architecture.

A APPENDIX

A.1 Architectural Details

We detail the architecture of LVTR in Fig. A.1. The overall design is similar to that of original transformer encoder-decoder. First, the transformer encoder processes video-text features, which are extracted from the backbone, added with temporal positional encoding² at each multi-head self-attention layer. Next, the decoder receives learnable proposals and encoder memory and process them with multiple multi-head self-attention and encoder-decoder attention layers. Finally, the output of decoder is used to generate the final set of predicted time segments, and also used to measure the correspondence between proposals and text queries.

A.2 Additional Experiments

Loss hyperparameters. We search for optimal loss hyperparameters in Table A.1. We begin by setting the loss coefficients to 1:1:1 by default. While set guidance loss (λ_{sg}) is essential for query identity matching, the temporal localization loss (λ_{L1} and λ_{iou}) directly affects the accurate video grounding. This can be confirmed by varying the coefficient for each term to 2 one-by-one. Among the three variations, we found that gIoU loss (λ_{iou}) is the most important term in the loss function. This is because the relative measure

²We use a fixed absolute encoding to represent the temporal positions.

Table A.1: Loss balancing parameters.

$\lambda_{L1}:\lambda_{iou}:\lambda_{sg}$	R1@0.5	R1@0.7	R5@0.5	R5@0.7	mIoU
1:1:1	53.39	30.79	80.68	60.76	51.24
2:1:1	56.42	31.59	78.90	63.03	52.77
1:2:1	58.03	31.23	78.02	60.49	52.15
1:1:2	57.41	32.91	77.09	57.49	53.50
1:3:1	49.59	28.03	66.81	48.78	48.18
1:3:2	58.79	33.38	77.47	59.68	53.00

Table A.2: Effect of the number of input frames.

#frames	R1@0.5	R1@0.7	R5@0.5	R5@0.7	mIoU
16	47.93	23.34	72.30	51.31	42.53
32	52.15	28.77	74.01	55.13	50.46
64	58.79	33.38	77.47	59.68	53.00
128	53.73	29.55	77.42	60.77	51.11
256	48.35	24.39	73.36	54.23	47.89

Table A.3: Effect of the number of input sentences.

#sentences	R1@0.5	R1@0.7	R5@0.5	R5@0.7	mIoU
2	33.86	17.31	70.41	44.00	38.73
3	46.15	22.03	81.58	63.17	47.05
4	58.79	33.38	77.47	59.68	53.00
5	35.41	17.51	69.19	48.74	39.58

is more robust to varying segments shifted over various time distributions. While maintaining the gIoU loss to hold the major term, 1:3:2 yields the best results in our setting.

Input analysis. In order to examine the effect according to the number of input video frames and the number of input sentences, we varied the numbers in Table A.2 and Table A.3, respectively. As we expect more frames to bring more temporal knowledge, too few frames miss the exact moment when the event occurs, leading to decrease in performance. However, the results reveal that a large number of frames does not always guarantees better results. This implies that adding more frames cause a trade-off in the optimization while increasing the sequence length. We found that 64 produces the best results. Using multiple sentences as input queries allows us to take advantage of the temporal contexts between language queries. In the R1 metric, using 4 sentences as an input outperforms using 3 sentences, while using 3 sentences as an input shows better results in the R5 metric. This is due to the fact that the average number of existing sentences in training split of *ActivityCaptions* is 3.739. We adopt 4 sentences as an input since we require a more accurate model on a stricter metric.

A.3 More Qualitative Results

To better see how LVTR understands the video contexts, we provide additional qualitative examples and contrast the success and failure cases in Fig. A.2. The results show that the LVTR successfully identifies the object described in the query and accurately localize the time segment, even if multiple objects appear in the video (row 1&2). Moreover, LVTR correctly reasons about the action that takes place from the first person point of view (row 3). Lastly, even if the same object appears repeatedly, LVTR distinguishes subtle contextual differences between them well (row 4). However, LVTR often fails to capture short-term events, especially when the object is too small (row 1&2). LVTR suffers when the time the event takes place is too long (e.g., whole video length) (row 3). Also, LVTR fails when the labeled time segment and the actual time segment where the query description matches the video content are significantly different (row 4).



Figure A.2: Qualitative examples of success and failure cases of LVTR on the *ActivityCaptions* dataset. The predicted time segment is considered correct only if it has sufficiently high IoU (i.e., $\text{IoU} > 0.5$) with ground truth time segment. Empty bars represent ground truths, and colored bars represent predictions.